RSC Advances

PAPER

View Article Online
View Journal | View Issue



Cite this: *RSC Adv.*, 2020, **10**, 24425

# Cu–Cd–Zn–S/ZnS core/shell quantum dot/polyvinyl alcohol flexible films for white light-emitting diodes†

Shenjie Li,* Tianyong Zha, Xiaoyu Gong, Qi Hu, Minghui Yu, Jinyu Wu, Ruolan Li, Jiaming Wang and Yanyan Chen*

We present a facile route for the synthesis of water-soluble Cu–Cd–Zn–S/ZnS core/shell quantum dots (QDs) by simple pH regulation. The PL spectra of Cu–Cd–Zn–S/ZnS core/shell quantum dots can cover the whole visible light region in the case of only two ratios of Cu/Cd/Zn. The emission wavelength of Cu–Cd–Zn–S/ZnS QDs can be conveniently tuned from 474 to 515 and 548 to 629 nm by adjusting the pH value when the ratios of Cu/Cd/Zn are fixed at 1 : 5 : 80 and 1 : 5 : 10, respectively. It is worth noting that under the condition of a constant Cu/Cd/Zn ratio, the UV-vis absorption spectra do not change with the fluorescence spectra, indicating that the band gap of QDs remains unchanged during the change of pH value. The photoluminescence (PL) quantum yield of the as-prepared QDs with yellow emission is up to 76%. The QDs also show excellent chemical stability after the deposition of the ZnS shell. Luminescent and flexible films are fabricated by combining Cu–Cd–Zn–S QDs with polyvinyl alcohol (PVA). The QD/PVA flexible hybrid films are successfully applied on top of a conventional blue InGaN chip for remote-type warm-white LEDs. As-fabricated warm-white LEDs exhibit a higher color rendering index (CRI) of about 89.2 and a correlated color temperature (CCT) of 4308 K.

Received 20th April 2020
Accepted 10th June 2020

DOI: 10.1039/d0ra03540h

rsc.li/rsc-advances



## 1. Introduction

With the increasing global energy consumption, people's concern about low cost and sustainable energy has been growing in recent years. Semiconductor quantum dot thin films (QDTFs) have attracted extensive interest owing to their high potential applications in quantum dot white light emitting diodes (WLEDs).[1–4] QDTFs can be fabricated by two main methods according to the reports in the literature. The first method involves the solution phase synthesis of QDs, post-purification, and coating QD solution.[5–10] Thus, a ligand exchange process and a tedious post-purification procedure are usually required. Additionally, QDTFs can be fabricated *via* a direct deposition method without the need of the complex quantum dot synthesis through molecular-based precursor solution.[11–15] Recently, we developed a molecular-based precursor solution approach to deposit Cu-doped $Zn_xCd_{1-x}S$ QD luminescent thin films with a PL quantum yield of 25.5%.[11] Wang *et al.* fabricated the Cu–In–Zn–S QDTFs though thermal decomposition of molecular-based precursors in the open air, and the PL quantum yields can reach as high as 22.1%.[15] However, these QDTFs were deposited onto a hard substrate, which is not suitable for flexible photoelectric devices. Thus, developing a synthetic approach for flexible QDTFs with the advantages of fold ability and crack resistance is of great significance.

Recently, high quality doped II–VI QDs such as Cu-doped ZnS, Cu-doped CdS and Cu-doped $Zn_xCd_{1-x}S$ QDs have been reported.[16–21] However, these QDs were usually synthesized by an organic phase approach which requires a high reaction temperature and large quantities of organic solvents. Lately, water-soluble $Cu^+$, $Ag^+$, $Au^+$-doped $Zn_xCd_{1-x}S$ QDs have been successfully synthesized by our group *via* aqueous thermal decomposition of Cu, Ag, Cd, Zn stock solutions through a hot-injection approach in a traditional three-neck flask.[22,23] However, the PL emission color of doped quantum dots is limited which is difficult to cover the entire visible range, impelling us to prepare full-color emitting Cu–Cd–Zn–S/ZnS QDs and investigate their PL properties. Since the emission peaks of these $Cu^+$-doped $Zn_xCd_{1-x}S$/ZnS and $Ag^+$-doped $Zn_xCd_{1-x}S$/ZnS QDs can be tuned from 466 to 612 nm by changing the Zn–Cd molar ratio, the $Cu^+$-doped $Zn_xCd_{1-x}S$/ZnS can form quaternary Cu–Cd–Zn–S QDs which are particularly interesting luminescent QDs since their emission can cover the entire visible light spectrum. In addition, the photoluminescence spectra of quantum dots can be extended to the near infrared region over 800 nm theoretically.

*School of Chemistry and Chemical Engineering, Hefei University of Technology, Hefei, Anhui, 230009, People's Republic of China. E-mail: shenjieli@hfut.edu.cn; yanyanchen@hfut.edu.cn; Fax: +86-563-3831302; Tel: +86-563-3831302*

† Electronic supplementary information (ESI) available. See DOI: 10.1039/d0ra03540h

In this article we present a green and facile route for synthesizing water-soluble Cu–Cd–Zn–S/ZnS core/shell QDs by simple pH regulation using inexpensive and low-toxic precursors. Compared with an organic phase approach, the aqueous phase approach is greener and milder, and these water soluble QDs show a high photoluminescence quantum yield (PLQY) of about 76% upon 380 nm excitation. More importantly, the emission color of QDs can be tuned in the whole visible light range by simple changing the pH value instead of adjusting the ratios of Cu/Cd/Zn, which is more facile than the tedious method of adjusting the proportion of cations to obtain different luminous colors. Semiconductor QDTFs are fabricated by combining polyvinyl alcohol (PVA) solution with Cu–Cd–Zn–S QDs, and flexible QDTFs has been successfully applied to a commercial blue InGaN chip for the remote-type WLEDs. Compared with WLED prepared with quantum dot powder, these flexible QDTFs overcome the reabsorption issue of QDs.[24–32] As-fabricated WLEDs exhibit a CIE color coordinate of (0.3499, 0.2860), a CCT of 4308 K, and a higher color rendering index (CRI) of about 89.2.

## 2. Experimental section

### 2.1 Chemicals

Copper chloride ($CuCl_2 \cdot 2H_2O$, 99.0%), zinc acetate ($Zn(OAc)_2 \cdot 2H_2O$, 99.0%), cadmium acetate ($Cd(OAc)_2 \cdot 2H_2O$, 99.0%), thiourea ($CH_4N_2S$, 99.0%), 3-mercaptopropionic acid (MPA, $HSCH_2CH_2COOH$, 98%) were purchased from Aladdin. Sodium hydroxide (NaOH, 96%), isopropyl alcohol ($C_3H_8O$, 99.7%) and sodium sulfide ($Na_2S \cdot 9H_2O$, 99.9%) were purchased from Beijing Chemical works. All chemicals were used as received without any further purification.

### 2.2 Preparation of stock solutions

Cu stock solution (0.2 M) was obtained by dissolving 0.68 g (4 mmol) of $CuCl_2 \cdot 2H_2O$ in 20.0 mL of de-ionized water. Cd stock solution (0.2 M) was prepared by dissolving 1.064 g (4.0 mmol) of $Cd(OAc)_2 \cdot 2H_2O$ in 20.0 mL of de-ionized water. Zn stock solution (0.2 M) was obtained by dissolving 0.878 g (4.0 mmol) of $Zn(OAc)_2 \cdot 2H_2O$ in 20.0 mL of de-ionized water at room temperature. $Na_2S$ stock solution (1.0 M) was prepared by dissolving 2.408 g (10.0 mmol) of $Na_2S \cdot 9H_2O$ in 10.0 mL of de-ionized water. ZnS shell stock solution (0.04 M) was obtained by dissolving 0.352 g (1.6 mmol) of $Zn(OAc)_2 \cdot 2H_2O$, 0.122 g (1.6 mmol) of thiourea in 40.0 mL of de-ionized water. 1.0 M NaOH aqueous solution was prepared by dissolving 1.600 g (40 mmol) of NaOH in 40.0 mL of de-ionized water.

### 2.3 Preparation of Cu–Cd–Zn–S QDs and Cu–Cd–Zn–S/ZnS core/shell QDs with different ratios

In a typical synthesis of Cu–Zn–Cd–S core quantum dots with the ratio of Cu : Cd : Zn (1/5/10), 0.05 mL of Cu stock solution (0.01 mmol), 0.25 mL of Cd stock solution (0.05 mmol), 0.5 mL of Zn stock solution (0.1 mmol), 0.031 g (0.64 mmol) of MPA and 15.0 mL of de-ionized water were loaded in a 50 mL beaker and the pH value was tuned to 5.5 with 1.0 M NaOH aqueous solution. Afterwards, 0.042 mL (0.155 mmol) of $Na_2S$ stock solution was injected into the beaker under magnetic stirring. Subsequently, the mixture was transferred to an autoclave and heated to 180 °C from room temperature and kept at this temperature for 30 min. Cu–Cd–Zn–S core QDs with different Cu/Cd/Zn ratios were synthesized by changing the volume ratio of Cu/Cd/Zn stock solution.

After the growth time of 30 min for the crude Cu–Cd–Zn–S core QDs, 0.192 mmol of ZnS shell stock solution and 0.384 mmol of MPA were loaded in the beaker to deposit ZnS shell around the Cu–Cd–Zn–S cores and the pH value was tuned to 5.5 with 1.0 M NaOH aqueous solution. Afterwards, the reaction lasted for 20 min at the same temperature.

### 2.4 Preparation of Cu–Cd–Zn–S QDs and Cu–Cd–Zn–S/ZnS core/shell QDs by adjusting the pH value

In a typical synthesis of Cu–Zn–Cd–S cores quantum dots with the ratio of Cu : Cd : Zn (1/5/10), 0.05 mL of Cu stock solution (0.01 mmol), 0.25 mL of Cd stock solution (0.05 mmol), 0.5 mL of Zn stock solution (0.1 mmol), 0.031 g (0.64 mmol) of MPA and 15.0 mL of de-ionized water were loaded in a 50 mL beaker and 0.042 mL (0.155 mmol) of $Na_2S$ stock solution was loaded in the beaker under magnetic stirring. The above solution is prepared in several copies. Afterwards, the pH value was tuned to different values with 1.0 M NaOH aqueous solution or MPA in different beakers. Subsequently, the mixture was transferred to an autoclave and heated to 180 °C from room temperature and kept at this temperature for 20 min.

After the growth time of 20 min for the crude Cu–Cd–Zn–S core QDs, 0.192 mmol of ZnS shell stock solution and 0.384 mmol of MPA were loaded in the beaker to deposit ZnS shell around the Cu–Cd–Zn–S cores and the pH value was tuned as same as precursor solution through 1.0 M NaOH aqueous solution or MPA. Afterwards, the reaction lasted for 20 min at the 180 °C.

### 2.5 Preparation of Cu–Cd–Zn–S/ZnS QD/PVA flexible hybrid films

For the preparation of 10 wt% PVA transparent solution, 5 g PVA and 45 g de-ionized water were loaded in a 100 mL beaker under magnetic stirring for 2 h on a 90 °C hot plate. In a typical procedure for the synthesis of Cu–Cd–Zn–S QD/PVA flexible hybrid films, Cu–Cd–Zn–S QDs were added to a 10 wt% PVA solution for 30 min at 60 °C (QD : PVA volume ratios of 1 : 1). Then, this clear and viscous Cu–Cd–Zn–S/ZnS QD/PVA solution was poured into a primary culture dish (diameter of 55 mm), and dried at room temperature. The QD/PVA flexible films were readily detached from the bottom of the culture dish.

### 2.6 Characterizations

For structural study, an X-ray diffractometer (Bruker Advance D8) was used. X-ray diffraction (XRD) patterns were measured in $2\theta$ range of 20–80° using Cu-K$\alpha$ radiation of wavelength $\lambda$ = 0.154 nm. UV-vis absorption spectra were measured by a TU-1901 spectrophotometer. Photoluminescence (PL) spectra were collected on a F96 pro Spectrofluorometer and the PL

 

intensity was calculated by integration of PL curve. High-resolution transmission electron microscopy (HR-TEM) images were taken on a FEI Tecnai G2 F20 operated at an accelerating voltage of 200 kV. The details of the characterization results are discussed below. The fluorescence decay curve was recorded by a Lecroy Wave Runner 6100 digital oscilloscope (1 GHz) using a tunable laser (pulse width = 4 ns, gate = 50 ns) as the excitation source (Continuum Sunlite OPO).The Commission Internationale de l'Eclairage (CIE) chromaticity color coordinates, color rendering index (CRI), and correlated color temperature (CCT) were measured by Stars pec SSP6612.

## 3. Results and discussion

An important property of QDs is that their emission spectra can be modulated in different ways. There are two main methods for regulating the fluorescence emission spectra of QDs in the literature. The first method is through size adjustment, such as CdS, CdSe and other binary QDs.[33–35] Additionally, PL emission spectra of multivariate QDs can be modulated by composition, such as Cu–In–S, Ag–In–S, and Cu–In–Zn–S.[36–38] Here, we developed an unusual method for the preparation of Cu–Cd–Zn–S/ZnS core/shell QDs with tunable emission colors by using NaOH aqueous solution or MPA to adjust the pH value in the precursor solution, because Cu–Cd–Zn–S system is particularly sensitive to pH value. The PL emission spectrum of Cu–Cd–Zn–S/ZnS core/shell QDs can be adjusted in a wide range under the same Cu/Cd/Zn ratio. Scheme 1 shows the fabrication strategy of Cu–Cd–Zn–S/ZnS core/shell QDs by adjusting the pH value. With the increase of pH value, the PL emission spectrum shows an obvious red shift. In this article, the luminescence color of the Cu–Cd–Zn–S/ZnS core/shell QDs were changed from blue to red by mainly changing the pH value.

Fig. 1(A) and (B) show PL spectra of Cu–Cd–Zn–S/ZnS core/shell QDs with different pH values at the excitation wavelength of 380 nm. PL spectra of Cu–Cd–Zn–S/ZnS core/shell quantum dots can cover whole visible light region in the case of only two ratios of Cu/Cd/Zn. The emission wavelength of Cu–Cd–Zn–S/ZnS QDs can be conveniently tuned from 474 to 515 nm and 548 to 629 nm by adjusting the pH value when the ratio of Cu/Cd/Zn is 1 : 5 : 10 and 1 : 5 : 80, respectively. The emission spectra of Cu–Cd–Zn–S/ZnS core/shell QDs can be tuned in the range of 474–629 nm, which almost covers the whole visible light region by simply changing the pH value. As-prepared QDs exhibit yellow emission with a photoluminescence (PL) quantum yield up to 75% after *in situ* depositing the ZnS shell over the Cu–Cd–Zn–S core quantum dots. It is worth mentioning that the QDs also show excellent chemical stability after the surface deposition of the ZnS shell. Fig. 1(C) and (D) show the UV-vis absorption Cu–Zn–Cd–S QDs with different pH value. The absorption spectra of alloyed Cu–Cd–Zn–S/ZnS core/shell QDs with different pH values remains almost the same, indicating that the band gap of the host material is independent of the pH value. The change of band gap mainly depends on its size and composition of QDs. Since only the pH value of Cu–Cd–Zn–S QDs has changed, the composition of precursor, reaction time, reaction temperature and other conditions have not changed, so the size and composition of Cu–Cd–Zn–S QDs have not changed. As a result, the band gap of quantum dot has not changed. This is particularly rare in other QDs reported in the literature.

The emission color of the Cu–Zn–Cd–S/ZnS core–shell QDs could be also tuned by changing the molar ratios of Cu/Cd/Zn. Fig. 2A shows PL spectra of Cu–Cd–Zn–S/ZnS core/shell QDs with different Cu/Cd/Zn ratios under the excitation wavelength of 380 nm. As shown in Fig. 2A, the emission wavelength of Cu–Cd–Zn–S/ZnS QDs can be conveniently tuned from 483 to 770 nm by adjusting the ratios of Cu/Cd/Zn. Note that the PL peak positions of Cu–Cd–Zn–S/ZnS core–shell QDs in Fig. 2A blue-shift with increasing Zn content and red-shift with increasing Cu and Cd contents (Fig. S1–S3†). The elemental ratios can significantly affect the optical band gap of Cu–Cd–Zn–S/ZnS QDs. A series of Cu–Cd–Zn–S/ZnS QDs with different compositions and band gaps could be obtained by changing the ratios of the starting materials. Since the band gap of ZnS (3.6 eV) is obviously larger than CdS (2.4 eV) and CuS (1.1 eV), when the content of Zn in Cu–Cd–Zn–S QDs gradually increases, the band gap of quantum dots will show a continuous blue shift in theory. Fig. 2B shows UV-vis absorption spectra of Cu–Cd–Zn–S/ZnS core/shell QDs synthesized by changing the molar ratios of the starting materials. As expected, a successive blue-shift of the

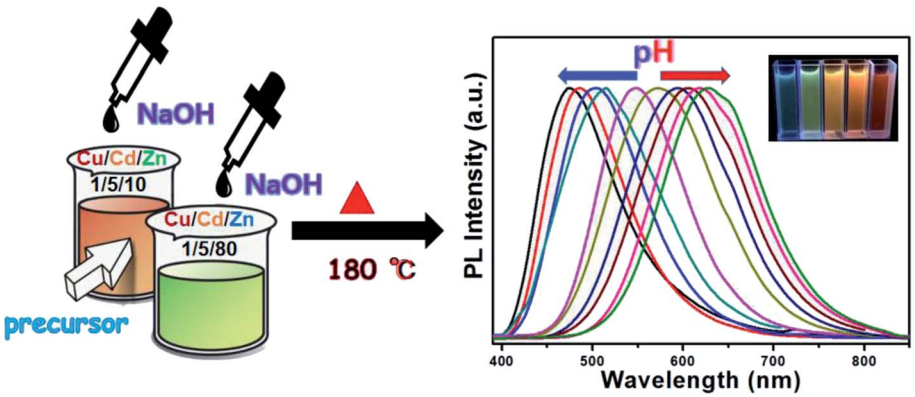


Scheme 1 Synthetic strategy of Cu–Cd–Zn–S/ZnS core/shell QDs by adjusting the pH value.

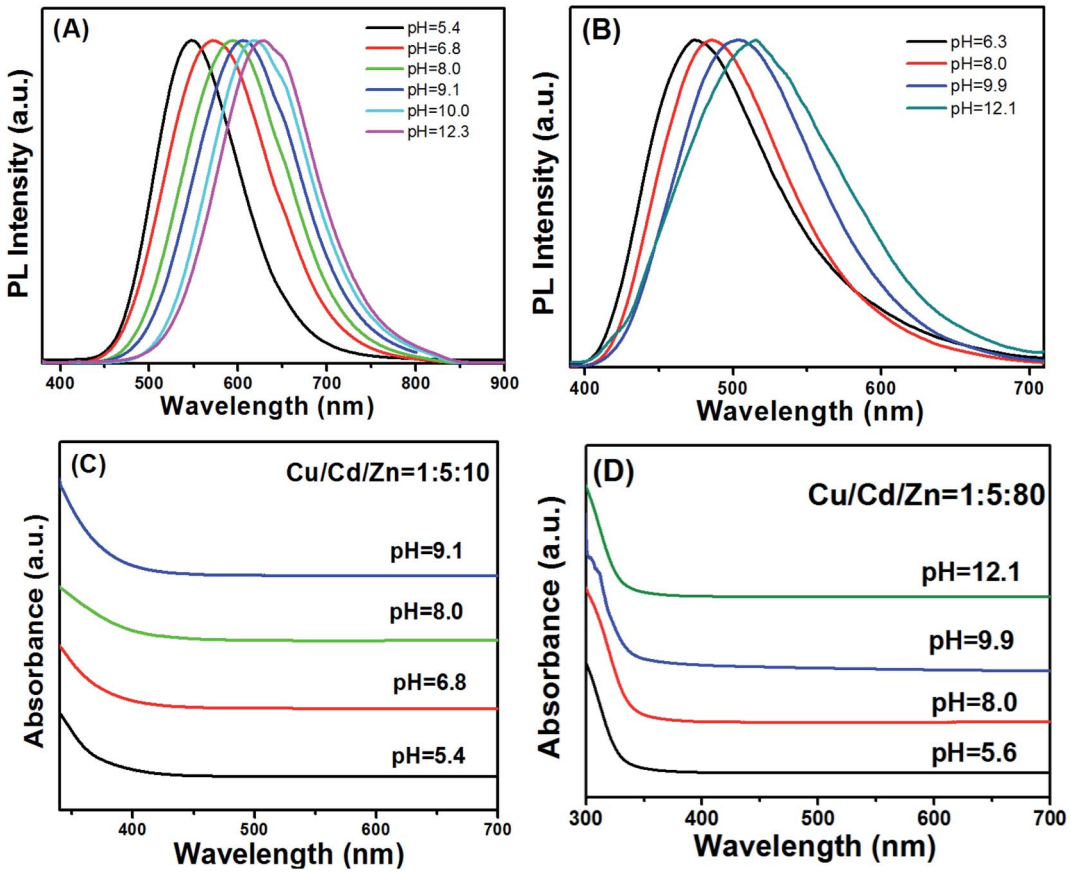


Fig. 1 Effect of pH on the fluorescence properties of Cu–Cd–Zn–S/ZnS core/shell QDs: PL emission spectra at the ratio of 1 : 5 : 10 and 1 : 5 : 80 (A and B) and their corresponding UV-vis absorption spectra of the ratio of 1 : 5 : 10 and 1 : 5 : 80 (C and D).

optical absorption band-edge was clearly observed with increasing the Zn content for Cu–Cd–Zn–S/ZnS QDs, indicating the formation of homogeneously alloyed Cu–Cd–Zn–S/ZnS QDs. Fig. 2C and D show the digital images of the Cu–Cd–Zn–S/ZnS core/shell QDs with different emission colors under sunlight and UV light irradiation.

Compared to PL spectra of Cu–Cd–Zn–S/ZnS core/shell QDs synthesized by changing pH value (474–629 nm) (Fig. S4†), PL spectra by changing the molar ratios of the starting materials can cover a wider range (483–770 nm). However, the preparation process of experimentation is very complex, and because there is a certain deviation between the actual metal ion ratios and starting precursor ratios, we need to conduct EDS characterization for each sample, which is tedious. The synthetic procedures of Cu–Cd–Zn–S/ZnS QDs *via* pH regulation is much simpler by comparison, which only needs to prepare the two ratios of Cu/Cd/Zn, and the PL spectra of Cu–Cd–Zn–S/ZnS core/shell QDs can almost cover the whole visible light region. It is noteworthy that the band gap of Cu–Cd–Zn–S/ZnS core/shell QDs will not change when the ratio of Cu/Cd/Zn is constant (Fig. 2A and B), which enable us to shift the emission wavelength of QDs without changing the band gap. This is especially suitable for some optoelectronic devices with band gap invariant and varying emission spectra.

Unlike $Cu^{+}$-doped $Zn_xCd_{1-x}S$ quantum dots, Cu–Cd–Zn–S core QDs exhibit relatively high PL QYs of 32% despite a lot of traps on the surface of the Cu–Cd–Zn–S core QDs. Here, we deposited the ZnS shell *in situ* over the Cu–Cd–Zn–S cores to build the type-I core–shell structure. Fig. S5A and S5B† show the evolution of the PL and UV-vis absorption spectra of Cu–Cd–Zn–S/ZnS core–shell QDs with different thickness ZnS shells starting from the Cu–Cd–Zn–S cores under an initial Cu : Cd : Zn ratio of 1 : 20 : 60. The growth of the ZnS shell did not change the emission and absorption spectra significantly. The PL peak positions of the Cu–Cd–Zn–S/ZnS core–shell QDs in Fig. S5A† do not significant shift with increasing the thickness of ZnS shell from 1 monolayer to 2 monolayers. However, PL peak position in Fig. S6A and S6B† have a certain degree of movement, it may be because the initial proportion of zinc ions in Fig. S6† is small, and obvious movement can be observed after Zn ion into core QDs, while the initial proportion of zinc in Fig. S5A† is relatively large, so the movement is not obvious. It was found that the PL QYs of Cu–Cd–Zn–S/ZnS core/shell QDs can reach as high as 76% after the growth of 2 monolayers of ZnS. In general, the PL QYs of the core–shell QDs could be enhanced more than 2 times greater than those of the cores, indicating that the surface recombination sites can be significantly removed using a wider band gap semiconductor as the

 

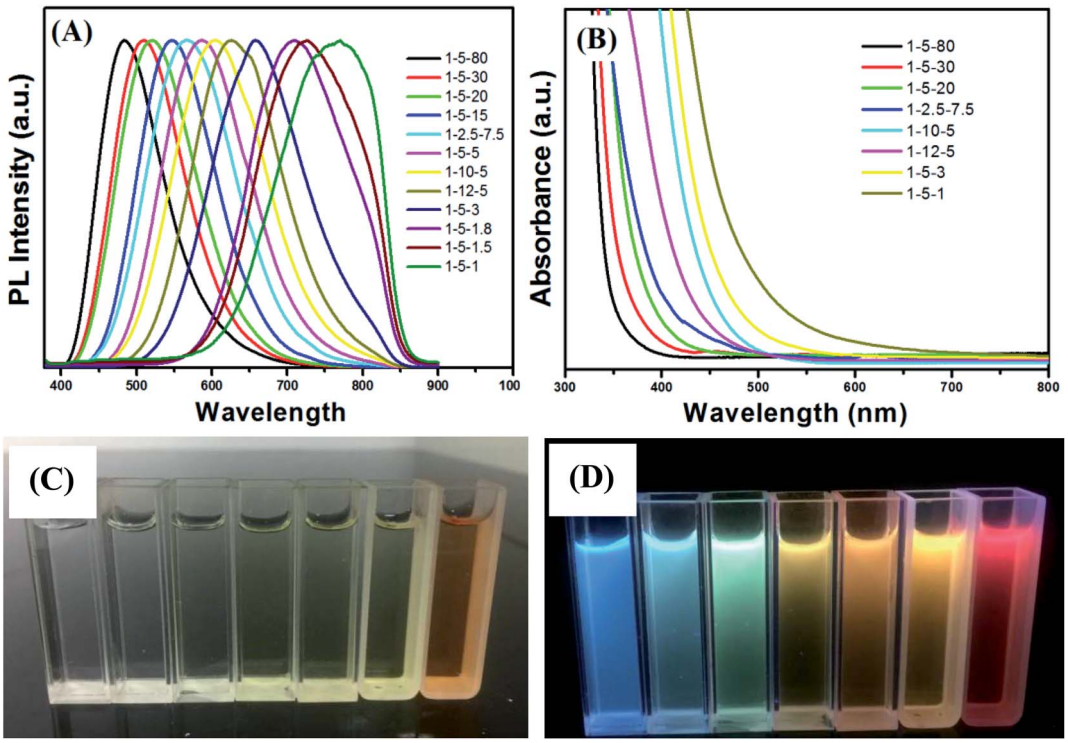


Fig. 2 PL spectra (A) and UV-vis absorption spectra (B) of Cu–Cd–Zn–S QDs with different ratios of Cu/Cd/Zn. The digital images of the Cu–Cd–Zn–S/ZnS core/shell QDs with different emission colors under sunlight (C) and UV light irradiation (D).

shell. The evolution of the PL spectra of different ratios of Cu/Cd/Zn showed the same rule (Fig. S6†).

Structural characterization of the Cu–Cd–Zn–S cores and the corresponding Cu–Cd–Zn–S/ZnS core/shell QDs were carried out by XRD (Fig. 3). Detailed analysis of the XRD data of cores and core/shell QDs revealed that both of them have the characteristics of a zinc-blende structure, which consists of three prominent peaks consistent with the (111), (220), and (311) planes. Due to the small size of quantum dots, the strength of the three peaks is relatively low, which is also a property of water-soluble quantum dots. After the deposition of the ZnS shell, the diffraction peak positions of Cu–Cd–Zn–S/ZnS core/shell QDs shift to higher angles, towards those of the standard zincblende ZnS, indicating the formation of the ZnS shell around the Cu–Cd–Zn–S cores QDs. Fig. S7† shows a series of XRD patterns of Cu–Cd–Zn–S QDs with different Cu/Cd/Zn ratios, and all QDs exhibit three broad diffraction peaks and similar half-peak width, confirming that the crystal structure and size of QDs do not change under different Cu/Cd/Zn ratios. As expected, the diffraction peaks of alloyed Cu–Cd–Zn–S QDs shift toward higher angle with an increase of Zn ratios, indicating that the lattice constants of alloys shrink. The size and size distribution are critically important for luminescent QDs. Fig. 4A and B show the high-resolution TEM (HR-TEM) images

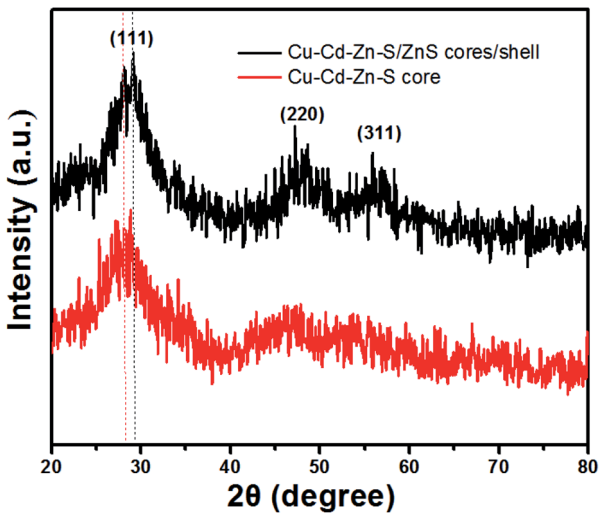


Fig. 3 XRD patterns of Cu–Cd–Zn–S core QDs with a Cu/Cd/Zn ratio of 1 : 5 : 10 and the corresponding Cu–Cd–Zn–S/ZnS core/shell QDs.

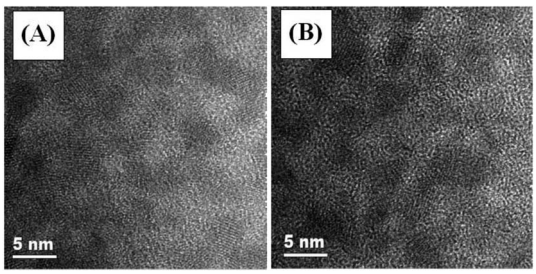


Fig. 4 HR-TEM images of Cu–Cd–Zn–S core QDs prepared under different Cu/Cd/Zn ratios: (A) 1 : 5 : 10 and (B) 1 : 5 : 80.

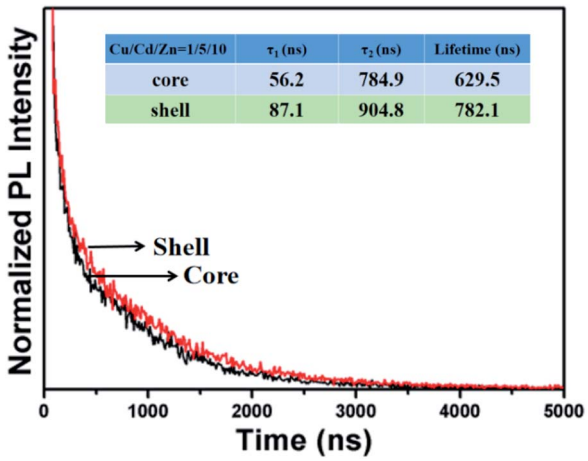


Fig. 5 Fluorescence decay curves of Cu–Cd–Zn–S core QDs and Cu–Cd–Zn–S/ZnS core/shell QDs.

of Cu–Cd–Zn–S QDs with a Cu/Cd/Zn ratio of 1 : 5 : 10 and 1 : 5 : 80. The TEM images in Fig. 4A and B demonstrate that both the QDs are well-dispersed, have an oval shape and a narrow size distribution. The Cu–Cd–Zn–S QDs have average diameter of ~3.3 nm and 3.5 nm with a standard deviation of around 6.5%, which is very close to the size calculated from the XRD pattern by the Scherrer equation.

Fig. 5 shows the PL decay curves of Cu–Cd–Zn–S core QDs and the corresponding Cu–Cd–Zn–S/ZnS core/shell with a Cu/Cd/Zn ratio of 1 : 5 : 10. In our experiments, all decay curves can be well fitted by a bi-exponential function: $I(t) = a\exp(-t/\tau_1) + b\exp(-t/\tau_2)$. As-prepared Cu–Cd–Zn–S core QDs exhibit an extremely long fluorescence lifetime of several hundreds of nanoseconds, which is independent of the composition and band gap of Cu–Cd–Zn–S core QDs. The calculated average PL decay lifetimes for Cu–Cd–Zn–S cores and Cu–Cd–Zn–S/ZnS core/shell QDs are 629 and 782 ns, respectively. The fitting results are listed in Table S1.† It is notable that the lifetime of Cu–Cd–Zn–S core and core/shell QDs is much longer than that of most carbon QDs, organic dyes and some II–VI, I–III–VI QDs.[3,25,39–41]

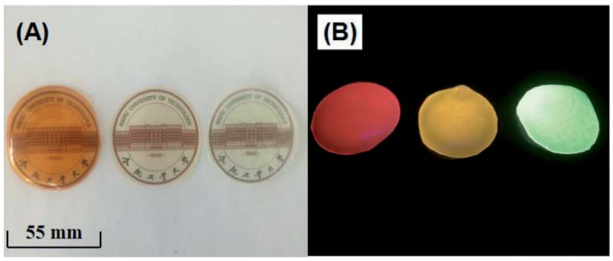


Fig. 7 The photographs of red, yellow and green luminescent films (QD : PVA ratios of 1 : 1) under sunlight (A) and UV irradiation (B).

The chemical compositions of Cu–Cd–Zn/S core QDs with different Cu/Cd/Zn ratios were determined by EDS. The elemental analysis results are listed in Table S2.† The results indicated that there was a tiny deviation between the actual metal ion ratios and starting precursor ratios. The metal/sulfide ratio is close to 1. In addition, the valence states of Cu, Cd, Zn and S in Cu–Cd–Zn–S core QDs were investigated by X-ray

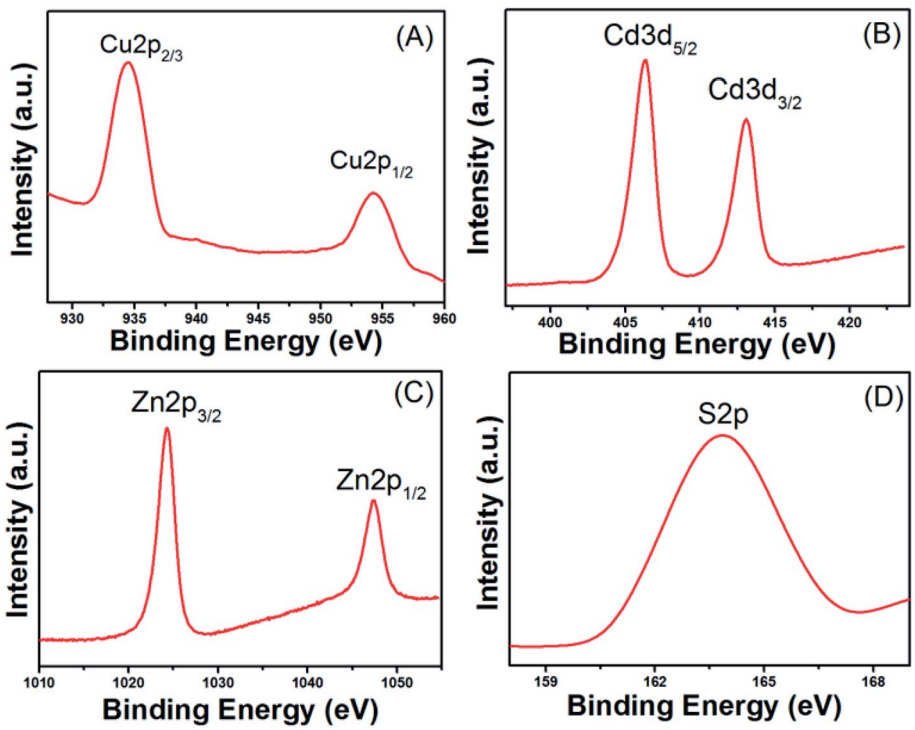


Fig. 6 XPS analysis of Cu–Cd–Zn–S (Cu/Cd/Zn = 1/5/10) core QDs: narrow-scan of the (A) Cu 2p, (B) Cd 3d, (C) Zn 2p and (D) S 2p region.

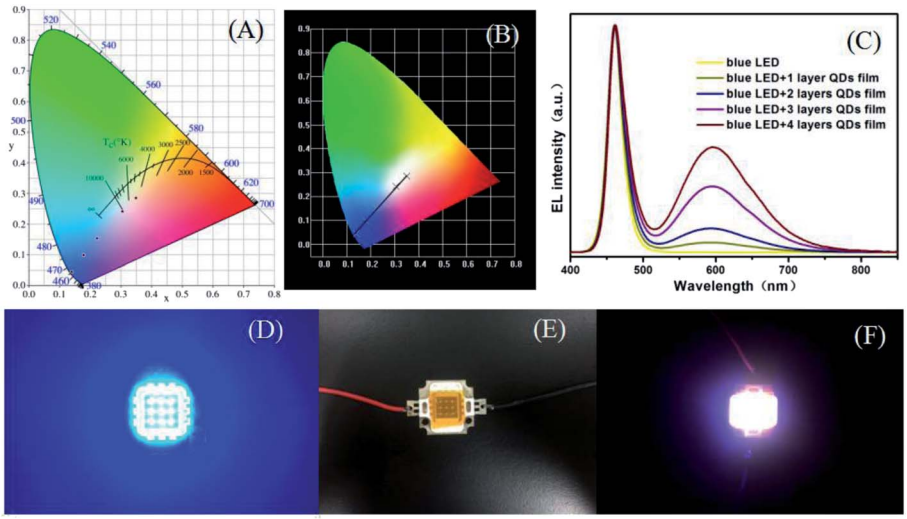


Fig. 8 (A) and (B) are the corresponding CIE chromaticity coordinates of orange QD/PVA film-based LEDs. (C) EL spectra of LEDs of QD/PVA films with various layers (at a drive current of 20 mA). The digital photograph of lighted blue LED (D), as-fabricated LEDs (E) and lighted white LED under the cover of Cu–Cd–Zn–S QDs/PVA films (F).

photoelectron spectroscopy (XPS) characterization. Six peaks corresponding to Cu $2p_{1/2}$, Cu $2p_{3/2}$, Cd $3d_{2/3}$, Cd $3d_{2/5}$, Zn $2p_{1/2}$ and Zn $2p_{3/2}$ were located at 934.4, 954.2, 406.3, 413.0, 1024.2, and 1047.3 eV (Fig. 6), suggesting that the valence states of Cu, Cd and Zn elements in the QDs are +1, +2 and +2, respectively. The peaks located at 163.7 eV were assigned to S 2p with a valence state of −2.

The preparation of uniform QD/polymer flexible films is a challenging task. The first reason is that conventional QDs are usually oil soluble and difficult to be dispersed uniformly in polymers. In addition, because of the features of the solid powder, the dispersion is usually not very uniform and it is easy to aggregation. For a successful QD/PVA film, the homogeneous dispersion of both QDs and PVA in the solution is the most important prerequisite. Here, the red, yellow and green water-soluble MPA-capped Cu–Cd–Zn–S/ZnS core/shell QD solutions were respectively mixed with PVA solution to form a uniform mixture solution, which was used to solve the agglomeration problem of the traditional QD powders in polymer matrix. Thus, homogeneous QD/PVA solutions can be obtained in a wide range of concentrations. Fig. 7A and B illustrate the photographs of red, yellow and green luminescent films (QD : PVA ratios of 1 : 1) under sunlight and UV irradiation, respectively, which exhibit high transmittance and homogeneous light emission. Not only that, the QD/PVA films we prepared is flexible and can remain flexible without breaking after 1000 times of bending, which has a broad application prospect in the field of flexible optoelectronic devices (Fig. S8†). The FT-IR spectra of red, yellow and green luminescent films (QD : PVA ratios of 1 : 1) are given in Fig. S9.† They exhibited a large quantity of characteristic bands including O–H stretching at 3350 $cm^{-1}$, C–H stretching at 2930 $cm^{-1}$ and the peak at 1462 $cm^{-1}$ is assigned to the bending frequencies of $–CH_2$. The above results demonstrated that the surfaces of the films were gathered with hydroxyl functional groups and carbon hydrogen bonds, resulting from PVA.

To evaluate the device performance for the synthesized QD/PVA flexible films, we fabricated white LEDs by combing blue chips (460 nm) with yellow-emitting QD/PVA film. The LEDs in the devices by using QD/PVA luminescent films of different layers, and the CIE chromaticity coordinates were shown in Fig. 8A and B. For the high uniform dispersion of QD/PVA luminescent films on the top of LEDs, our devices show uniform color distribution, which are more advantageous than LEDs using bulk phosphor/QD powders/resin as wavelength converter. The EL spectra of the devices were measured and are displayed in Fig. 8C. The sharp emission band at 460 nm is ascribed to a blue InGaN chip. The four broad emission bands centered at 596 nm correspond to layer 1 to layer 4, and the CCTs under an operating current of 20 mA are 5105, 6472, 9423 and 4308 K, respectively. The corresponding CIE index marked in CIE 1931 color spaces are (0.1792, 0.0.0987), (0.2222, 0.1534), (0.3053, 0.2417) and (0.3499, 0.2860) (see Fig. 8A and B). The emitting colors of LEDs changed from blue to bluish-purple, caesious, white and warm-white, respectively. Photographs of lighted blue-LED, as-fabricated LEDs and lighted WLED are shown in Fig. 8D–F. Using the QD/PVA luminescent films of different layers, the CCT decreases from 9423 to 4308 K. Warm-white lights are successfully created with five layers. More importantly, our QD/PVA films were prepared in aqueous phase, which is more cost-effective and greener.

## 4. Conclusions

In summary, we have successfully synthesized highly luminescent Cu–Cd–Zn–S/ZnS core/shell QDs by simple pH regulation. The Cu–Cd–Zn–S/ZnS core/shell QDs show high PLQYs of 76% and the PL spectra can cover whole visible light region in the case of only two ratios of Cu/Cd/Zn. Under the condition of

constant Cu/Cd/Zn ratio, the UV-vis absorption spectrum does not move with the change of fluorescence spectrum. Luminescent and flexible films are fabricated by combining Cu–Cd–Zn–S QDs with PVA. The QD/PVA films are successfully applied on top of a conventional blue InGaN chip for remote-type warm-white LEDs. As-fabricated warm-white LEDs exhibit a higher color rendering index (CRI) of about 89.2 and a correlated color temperature (CCT) of 4308 K. These results indicate that as-prepared core/shell QDs are promising luminescent materials for blue LED-pumped white LEDs.

## Conflicts of interest

There are no conflicts to declare.

## Acknowledgements

This work was supported by Natural Science Foundation of Anhui Province (Grant No. 1808085ME111), National Natural Science Foundation of China (Grant No. 51502070), the Fundamental Research Funds for the Central Universities (Grant No. JZ2019YYPY0032). The Undergraduate Innovation and Entrepreneur-ship Training Program (Grant No. S202010359349).

## References

1 X. Dai, Z. Zhang, Y. Jin, Y. Niu, H. Cao, X. Liang, L. Chen, J. Wang and X. Peng, Solution-processed, high-performance light-emitting diodes based on quantum dots, *Nature*, 2014, **515**, 96–99.

2 X. Kang, T. Yang, L. Wang, S. Wei and D. Pan, Warm White Light Emitting Diodes with Gelatin-Coated $AgInS_2$/ZnS Core/Shell Quantum Dots, *ACS Appl. Mater. Interfaces*, 2015, **7**, 27713–27719.

3 L. Wang, X. Kang and D. Pan, High color rendering index warm white light emitting diodes fabricated from $AgInS_2$/ZnS quantum dot/PVA flexible hybrid films, *Phys. Chem. Chem. Phys.*, 2016, **18**, 31634–31639.

4 H. Zhang, W. Fang, Y. Zhong and Q. Zhao, Zn-Ag-In-S quantum dot sensitized solar cells with enhanced efficiency by tuning defects, *J. Colloid Interface Sci.*, 2019, **547**, 264–274.

5 P. Anikeeva, J. Halpert, M. Bawendi and V. Bulovic, Electroluminescence from a mixed red- green-blue colloidal quantum dot monolayer, *Nano Lett.*, 2007, **7**, 2196–2200.

6 J. Tang, H. Liu, D. Zhitomirsky, S. Hoogland, X. Wang, M. Furukawa, L. Levina and E. Sargent, Quantum junction solar cells, *Nano Lett.*, 2012, **12**, 4889–4894.

7 J. Schornbaum, Y. Zakharko, M. Held, S. Thiemann, F. Gannott and J. Zaumseil, Light-emitting quantum dot transistors: emission at high charge carrier densities, *Nano Lett.*, 2015, **15**, 1822–1828.

8 L. Korala, Z. Wang, Y. Liu, S. Maldonado and S. Brock, Uniform thin films of CdSe and CdSe (ZnS) core (shell) quantum dots by sol-gel assembly: enabling photoelectrochemical characterization and electronic applications, *ACS Nano*, 2013, **7**, 1215–1223.

9 R. Liang, R. Tian, W. Shi, Z. Liu, D. Yan, M. Wei, D. Evans and X. Duan, A temperature sensor based on CdTe quantum dots-layered double hydroxide ultrathin films via layer-by-layer assembly, *Chem. Commun.*, 2013, **49**, 969–971.

10 Q. Zhang, J. Jie, S. Diao, Z. Shao, Q. Zhang, L. Wang, W. Deng, W. Hu, H. Xia, X. Yuan and S. Lee, Solution-processed graphene quantum dot deep-UV photodetectors, *ACS Nano*, 2015, **2**, 1561–1570.

11 Y. Chen, S. Li, L. Huang and D. Pan, Single-step direct fabrication of luminescent Cu-doped $Zn_xCd_{1-x}S$ quantum dot thin films via a molecular precursor solution approach and their application in luminescent, transparent, and conductive thin films, *Nanoscale*, 2014, **6**, 9640–9645.

12 Q. Tian, G. Wang, W. Zhao, Y. Chen, Y. Yang, L. Huang and D. Pan, Versatile and Low-Toxic Solution Approach to Binary, Ternary, and Quaternary Metal Sulfide Thin Films and Its Application in $Cu_2ZnSn(S,Se)_4$ Solar Cells, *Chem. Mater.*, 2014, **26**, 3098–3103.

13 Y. Chen, J. Min, Q. Wang and S. Li, Metal sulfide precursor aqueous solutions for fabrication of Ag-doped $Zn_xCd_{1-x}S$ quantum dots thin films, *J. Lumin.*, 2016, **180**, 258–263.

14 S. Li, T. Zha, Q. Wang, C. Wang, Y. Ren, Y. Chen and D. Pan, Facile fabrication of p-type CuxS transparent conducting thin films by metal sulfide precursor solution approach and their application in quantum dot thin films, *J. Alloys Compd.*, 2017, **716**, 278–283.

15 L. Wang, X. Kang, L. Huang and D. Pan, Temperature-dependent photoluminescence of cadmium-free Cu-Zn-In-S quantum dot thin films as temperature probes, *Dalton Trans.*, 2015, **44**, 20763–20768.

16 B. Srivastava, S. Jana and N. Pradhan, Doping Cu in Semiconductor Nanocrystals: Some Old and Some New Physical Insights, *J. Am. Chem. Soc.*, 2011, **133**, 1007–1015.

17 S. Sarkar, N. Karan and N. Pradhan, Ultrasmall Color-Tunable Copper-Doped Ternary Semiconductor Nanocrystal Emitters, *Angew. Chem., Int. Ed.*, 2011, **50**, 6065–6069.

18 D. Chen, R. Viswanatha, G. Ong, R. Xie, M. Balasubramaninan and X. Peng, Temperature Dependence of "Elementary Processes" in Doping Semiconductor Nanocrystals, *J. Am. Chem. Soc.*, 2009, **131**, 9333–9339.

19 X. Zhang, X. Zhou and X. Zhong, One-Pot Noninjection Synthesis of Cu-Doped $Zn_xCd_{1-x}S$ Nanocrystals with Emission Color Tunable over Entire Visible Spectrum, *Inorg. Chem.*, 2012, **51**, 3579–3587.

20 S. Sarkar, B. Patra, A. Guria and N. Pradhan, The Redox Chemistry at the Interface for Retrieving and Brightening the Emission of Doped Semiconductor Nanocrystals, *J. Phys. Chem. Lett.*, 2013, **4**, 2084–2090.

21 C. Unni, D. Philip, S. Smitha, K. Nissamudeen and G. Gopchandran, Aqueous synthesis and characterization of CdS, CdS:$Zn^{2+}$ and CdS:$Cu^{2+}$ quantum dots, *Spectrochim. Acta, Part A*, 2009, **72**, 827–832.

 

22 Y. Chen, L. Huang, S. Li and D. Pan, Aqueous synthesis of glutathione-capped $Cu^+$ and $Ag^+$ -doped $Zn_xCd_{1-x}S$ quantum dots with full color emission, *J. Mater. Chem. C*, 2013, **1**, 751–756.

23 Y. Chen, S. Li, L. Huang and D. Pan, Novel $Au^+$-doped $Zn_xCd_{1-x}S$/ZnS core/shell quantum dots, *Mater. Res. Express*, 2014, **1**, 015033.

24 S. Park, A. Hong, J. Kim, H. Yang, K. Lee and H. Jang, Highly Bright Yellow-Green-Emitting $CuInS_2$ Colloidal Quantum Dots with Core/Shell/Shell Architecture for White Light-Emitting Diodes, *ACS Appl. Mater. Interfaces*, 2015, **7**, 6764–6771.

25 X. Kang, Y. Yang, L. Huang, Y. Tao, L. Wang and D. Pan, Large-scale synthesis of water-soluble $CuInSe_2$/ZnS and $AgInSe_2$/ZnS core/shell quantum dots, *Green Chem.*, 2015, **17**, 4482–4488.

26 H. Yoon, J. Oh, M. Ko, H. Yoo and Y. Do, Synthesis and characterization of green Zn-Ag-In-S and red Zn-Cu-In-S quantum dots for ultrahigh color quality of down-converted white LEDs, *ACS Appl. Mater. Interfaces*, 2015, **7**, 7342–7350.

27 D. Jo and H. Yang, Synthesis of highly white-fluorescent Cu-Ga-S quantum dots for solid-state lighting devices, *Chem. Commun.*, 2016, **52**, 709–712.

28 X. Yuan, R. Ma, W. Zhang, J. Hua, X. Meng, X. Zhong, J. Zhang, J. Zhao and H. Li, Dual emissive manganese and copper co-doped Zn-In-S quantum dots as a single color-converter for high color rendering white-light-emitting diodes, *ACS Appl. Mater. Interfaces*, 2015, **7**, 8659–8666.

29 B. Chen, H. Zhong, M. Wang, R. Liu and B. Zou, Integration of $CuInS_2$-based nanocrystals for high efficiency and high color rendering white light-emitting diodes, *Nanoscale*, 2013, **5**, 3514–3519.

30 C. Ruan, Y. Zhang, M. Lu, C. Ji, C. Sun, X. Chen, H. Chen, V. Colvin and W. Yu, White light-emitting diodes based on $AgInS_2$/ZnS quantum dots with improved bandwidth in visible light communication, *Nanomaterials*, 2016, **6**, 13.

31 A. Aboulaich, M. Michalska, R. Schneider, A. Potdevin, J. Deschamps, R. Deloncle, G. Chadeyron and R. Mahiou, Ce-Doped YAG Nanophosphor and Red Emitting $CuInS_2$/ZnS Core/Shell Quantum Dots for Warm White Light-Emitting Diode with High Color Rendering Index, *ACS Appl. Mater. Interfaces*, 2014, **6**, 252–258.

32 J. Kim and H. Yang, White lighting device from composite films embedded with hydrophilic Cu(In, Ga)$S_2$/ZnS and hydrophobic InP/ZnS quantum dots, *Nanotechnology*, 2014, **22**, 225601.

33 D. Pan, X. Ji, L. An and Y. Lu, Observation of Nucleation and Growth of CdS Nanocrystals in a Two-Phase System, *Chem. Mater.*, 2008, **20**, 3560–3566.

34 D. Pan, Q. Wang, S. Jiang, X. Ji and L. An, Synthesis of Extremely Small CdSe and Highly Luminescent CdSe/CdS Core-Shell Nanocrystals via a Novel Two-Phase Thermal Approach, *Adv. Mater.*, 2005, **17**, 176–179.

35 D. Pan, S. Jiang, L. An and B. Jiang, Controllable Synthesis of Highly Luminescent and Monodisperse CdS Nanocrystals by a Two-Phase Approach under Mild Conditions, *Adv. Mater.*, 2004, **16**, 982–985.

36 Y. Chen, Q. Wang, T. Zha, J. Min, J. Gao, C. Zhou, J. Li, M. Zhao and S. Li, Green and facile synthesis of high-quality water-soluble Ag-In-S/ZnS core/shell quantum dots with obvious bandgap and sub-bandgap excitations, *J. Alloys Compd.*, 2018, **753**, 364–370.

37 Y. Chen, S. Li, L. Huang and D. Pan, Green and Facile Synthesis of Water-Soluble Cu-In-S/ZnS Core/Shell Quantum Dots, *Inorg. Chem.*, 2013, **52**, 7819–7821.

38 S. Li, Y. Chen, L. Huang and D. Pan, Simple continuous-flow synthesis of Cu-In-Zn-S/ZnS and Ag-In-Zn-S/ZnS core/shell quantum dots, *Nanotechnology*, 2013, **24**, 395705–395710.

39 C. Sun, Y. Zhang, K. Sun, C. Reckmeier, T. Zhang, X. Zhang, J. Zhao, C. Wu, W. Yu and A. Rogach, Combination of carbon dot and polymer dot phosphors for white light-emitting diodes, *Nanoscale*, 2015, **7**, 12045–12050.

40 S. Zhu, Q. Meng, L. Wang, J. Zhang, Y. Song, H. Jin, K. Zhang, H. Sun, Y. Wang and B. Yang, Highly Photoluminescent Carbon Dots for Multicolor Patterning, Sensors, and Bioimaging, *Angew. Chem., Int. Ed.*, 2013, **52**, 3953–3957.

41 T. Nguyen, W. Hamad and M. MacLachlan, CdS quantum dots encapsulated in chiral nematic mesoporous silica: new iridescent and luminescent materials, *Adv. Funct. Mater.*, 2014, **24**, 777–783.